ELSEVIER

Biophysical Chemistry 65 (1997) 189–204

Biophysical Chemistry

pK_a calculations along a bacteriorhodopsin molecular dynamics trajectory

Lars Sandberg, Olle Edholm

Theoretical Physics, Royal Institute of Technology, S-100 44 Stockholm 70, Sweden

Received 24 September 1996; accepted 4 December 1996

Abstract

Electrostatic calculations of pK_a-values are reported along a 400 ps molecular dynamics trajectory of bacteriorhodopsin. The sensitivity of calculated pK_a values to a number of structural factors and factors related to the modelling of the electrostatics are also studied. The results are very sensitive to the choice of internal dielectric constant of the protein (in the interval 2–4). Moreover it is important to include internal water molecules and to average over a long enough portion ($\sim$ 100 ps) of an equilibrium molecular dynamics trajectory. The internal waters are necessary to get an ion-counter ion complex with the Schiff base and Arg 82 protonated and the aspartic groups (85 and 212) deprotonated. The fluctuations along the MD-trajectory do not change the protonation state of internal residues at neutral pH. However, at other pH values the averaging along a trajectory maybe crucial to get correct protonation states. A relationship is found between the arginine group 82, the aspartic group 85 and the glutamate group 204. Glu 204 is protonated in the ground state but the pK_a value decreases towards deprotonation when the chromophore isomerizes into the *cis* state. © 1997 Elsevier Science B.V.

Keywords: Electrostatics; Fluctuations; Internal water; Protonation; Poisson–Boltzmann; FDPB method

1. Introduction

Electrostatic calculations using the Poisson and Poisson–Boltzmann equation have been performed with some success on proteins for almost ten years (see e.g. [1–3]). The aim is to calculate differences in free energy between states with different protonation and from that to predict pK_a values.

The protonation state of bacteriorhodopsin (bR) has already been studied by this kind of theoretical method in two articles [4,5]. Both show that despite the approximations employed and the fairly low resolution of the cryo electron microscopy structure [6], protonation states of the internal titratable residues can be calculated that agree with available experimental information. Still, the pK_a values differed typically by 5–10 units due to the employment of different approximations. The major improvement in the Sampogna and Honig article [5] as compared to that of Bashford and Gerwert [4] is the inclusion of some internal water molecules that were put into the experimental structure using simple modelling. Further, calculations were also performed on the protein with the chromophore in the *cis* state. On the other hand Bashford and Gerwert based their calculation on 20 structures, which were energy minimized from a 20 ps high temperature molecular dynamics trajectory while Sampogna and Honig use one single

PII S0301-4622(96)02262-4

rigid structure. Bashford and Gerwert [4] find an important effect from turning the side chain of Arg 82 upwards towards the Schiff base. Sampogna and Honig [5] also try this, but then lack space for internal water in the Schiff base region. Further, Bashford and Gerwert included a mixed environment with dielectric constant 4 (membrane) and 80 (water) while Sampogna and Honig used a uniform surrounding with a dielectric constant of 80. In both cases the loops, which are not resolved in the structure of Henderson, were not present.

The possibility of using electrostatic calculations of this type to shed light on the mechanism for the light driven proton transfer across the membrane that is performed by bR has been addressed by Engels et al. [7] and Scharnagl et al. [8]. The transport is accomplished through protonation and deprotonation of residues along the proton pathway in the protein by a process that is initiated by a *trans/cis* conformational change in the chromophore. However, the results from these studies are yet far from conclusive.

The results also showed a sensitivity to details in the structure close to the titratable sites. This sensitivity should be expected since some of the titratable residues changes protonation state during the photocycle due to fairly small structural changes. This makes the problem even more interesting and challenging. Therefore, it is not out of place to present another article studying the same protein with the same methods (in fact we are using Bashfords program). We add to the two earlier articles a more systematic study of the sensitivity to different approximations and studies based on an equilibrium molecular dynamics simulations (including a few internal water molecules). We then find that the internal waters are essential and that results are sensitive to details of the structure. This indicates that it is not enough to consider one single structure as Sampogna and Honig [5] do and that it is not sufficient to neglect the internal water as Bashford and Gerwert [4] do. Other possible approximations as neglecting loops, to use a uniform environment with high dielectric constant and to neglect the influence of counter ions seems to have less effect on the interior residues. Our calculations are based on structures from 400 ps of molecular dynamics calculations obtained after 100 ps of equilibration including the internal water molecules. We find pK_a values that in general seem to be in between those of the two earlier articles. Since we base our results on a fairly long molecular dynamics trajectory, we are also able to estimate fluctuations and from that the statistical errors in the pK_a values.

2. Theory and methods

The main objective here is to describe the dynamic properties of active membrane transporters, in particular bacteriorhodopsin (bR). The understanding of proton transfer reaction and acidity of the protein components is essential to either modelling of, or to attempting to simulate, parts of or entire transport cycles. In order to find the protonation state of important interior residues we apply the continuum dielectric model [9].

The protonation state s of the totally deprotonated titratable site protein A with N titratable sites is represented by a N-dimensional vector $\bar{\delta}^s$, which elements δ_i^s equals 1 or 0 due to whether the site i is protonated [p] or unprotonated [u]. The chemical reaction to form a specific protonation state $\bar{\delta}^s$ of A is:

$$A + \nu(\bar{\delta}^s)H \overset{\Delta G(\bar{\delta}^s)}{\rightarrow} AH_\nu(\bar{\delta}^s) \qquad (1)$$

where $\nu(\bar{\delta}^s)$ is the required number of protons and $\Delta G(\bar{\delta}^s)$ is the standard free energy of the reaction [10]. The $\Delta G(\bar{\delta}^s)$ is expressed in a composition of protonation free energies $\Delta G_{i,(p)}$ of site i in the protein phase (p), where

$$\begin{aligned}\Delta G_{i,(p)} &= \Delta G_{i,(aq)} + \Delta(\Delta G_{solv})_i + \Delta(\Delta G_{back})_i + (\Delta G_{tcc})_i \\ &= 2.303 k_B T(pK_{intr})_i + (\Delta G_{tcc})_i. \qquad (2)\end{aligned}$$

We abbreviate $\Delta G_{i,(aq)}$ as the free energy of protonation that the site compound, e.g. a blocked single amino acid side chain, has in the aqueous phase. The remaining part is represented by dividing it into a reaction field term $\Delta(\Delta G_{solv})_i$, an interaction term $\Delta(\Delta G_{back})_i$ between the site compound charges and non titrating backgound (partial) charges, e.g. the backbone dipoles, and finally a term due to the titratable sites charge–charge interaction $(\Delta G_{tcc})_i$

[3,4,11]. The last term consequently only emerges from the protein phase, and is awkward since the other titrating site charges are themselves pH dependent. On the second line the intrinsic pK_a of site i, $(pK_{intr})_i$, is introduced [12]. It is defined as the pK_a the site compound will have if it is the only titratable group inside the protein.

To evaluate the above presented free energy terms one could hypothesize that they are primarily made up of electrostatic contributions. However some cautiousness is necessary since the protein structure itself is determined by atomic interactions. Accordingly a change of the protonation state will affect the protein structure, in most cases insignificantly. These small transformations may still be problematical, since the electrostatic energy, the pK_a values and the titration curves are all very sensitive, as to be verified hereunder.In the continuum model, the heterogeneous dielectric protein is represented by a low relative permittivity $\epsilon_{protein}$. The surrounding aqueous solvent has a high dielectric constant of 80. The free energy terms are estimated by calculating the work of charging in the protein phase (p) in comparison with the aqueous phase (aq).The site compound consists of M discrete point charges q_μ, where $\mu = 1, 2, 3, \ldots, M$, at the atomic nuclei positions $\boldsymbol{r}_\mu$. The electrostatic potential field $\phi(\boldsymbol{r})$ satisfies the Poisson equation:

$$\nabla \cdot \epsilon(\boldsymbol{r})\epsilon_0 \nabla\phi(\boldsymbol{r}) = -\rho(r), \tag{3}$$

where the site compound charge density is $\rho(\boldsymbol{r}) = \Sigma q_\mu \delta(\boldsymbol{r} - \boldsymbol{r}_\mu)$. By a Green's functions approach the solution within the protein is

$$\phi(\boldsymbol{r}, q_1, \ldots, q_M) = \frac{1}{4\pi\epsilon} \sum_{\mu=1}^{M-1} \frac{q_\mu}{\|\boldsymbol{r} - \boldsymbol{r}_\mu\|} + \phi^*(\boldsymbol{r}, q_1, \ldots, q_M). \tag{4}$$

The potential ϕ is a combination of Coulomb terms and a reaction field potential ϕ^* due to the dielectric interface. The latter may for simple geometric forms be expressed by multipole expansion and by the use of image approximation [13–15]. The fields are calculated with only the charges of the titrating site i under consideration present. Consequently there are four different potential fields to compute, i.e. for the unprotonated site compound: $\phi^{[u]}_{(p)}; \phi^{[u]}_{(aq)}$, and for the protonated state: $\phi^{[p]}_{(p)}; \phi^{[p]}_{(aq)}$. The electrostatic potential energy of the protonated site compound in the protein phase is

$$W^{[p]}_{(p)} = \frac{1}{2}\int_V \rho^{[p]}(\boldsymbol{r})\,\phi^{[p]}_{(p)}(\boldsymbol{r})\,d^3r = \frac{1}{2}\sum_{\mu=1}^{M} q^{[p]}_\mu \phi^{[p]}_{(p)}(\mathbf{r}_\mu). \tag{5}$$

The same procedure gives the remaining three charging terms

$$\begin{cases} (\Delta G_{solv})^{[p]}_i = W^{[p]}_{(p)} - W^{[p]}_{(aq)} = \frac{1}{2}\sum_{\mu=1}^{M} q^{[p]}_\mu \left(\phi^{*[p]}_{(p)} - \phi^{*[p]}_{(aq)}\right) \\ (\Delta G_{solv})^{[u]}_i = W^{[u]}_{(p)} - W^{[u]}_{(aq)} = \frac{1}{2}\sum_{\mu=1}^{M} q^{[u]}_\mu \left(\phi^{*[u]}_{(p)} - \phi^{*[u]}_{(aq)}\right). \end{cases}$$

$$\Delta(\Delta G_{solv})_i = (\Delta G_{solv})^{[p]}_i - (\Delta G_{solv})^{[u]}_i \tag{6}$$

The Coulomb terms cancel in the subtraction, since they are independent of the external dielectric constant and the geometry of the dielectric boundary [3,4]. If different structures are compared, a word of warning is appropriate. Then there may be other important contributions to the free energy difference than electrostatic energies. For instance, entropic changes may contribute to the free energy alteration which will give a much more difficult problem.

The interaction term $\Delta(\Delta G_{back})_i$ is expressed in the above deduced potential fields, originating from the site compound. The term is equal to the difference in potential energy of the non titrating background charges in the electrostatic fields, i.e.

$$\begin{aligned} \Delta(\Delta G_{back})_i &= (\Delta G_{back})_{i,(p)} - (\Delta G_{back})_{i,(aq)} \\ &= W'^{[p]}_{(p)} - W'^{[u]}_{(p)} - W'^{[p]}_{(aq)} + W'^{[u]}_{(aq)}. \end{aligned} \tag{7}$$

With more than one titratable site there will be an extra free energy contribution $(\Delta G_{tcc})_i$, due to the mutual site charge interactions. This term is determined by the protonation states of the other sites, thereby being pH-dependent. $(\Delta G_{tcc})_i$ is defined by the symmetric matrix $W = (w_{ij})$, where w_{ij} is the electrostatic interaction between unit charges placed at site i and j. The diagonal elements w_{ii} are all zero, since the self-energies are a constituent part of the intrinsic free energy term.

By combining the results the standard free energy $\Delta G(\bar{\delta}^s)$ of reaction (1) is:

$$\Delta G(\bar{\delta}^s) = 2.303 k_B T \sum_{i=1}^{N} (pK_{intr})_i \delta_i^s + \frac{1}{2} \sum_{i=1}^{N} \sum_{j=1}^{N} w_{ij}(q_i^0 + \delta_i^s)(q_j^0 + \delta_j^s). \quad (8)$$

The charge q_i^0 is that of the unprotonated state of site i (single point titration site model). The first term to the right is the intrinsic energy of adding ν protons, and the second term is the total site interaction energy of the $\bar{\delta}^s$ protein state.

The fractional degree of protonation of site i, f_i, is determined by a statistical mechanical average of the site protonation state δ_i^s over all the system's accessible protonation states s. With N titratable sites, there are 2^N possible states and thus

$$f_i = \langle \delta_i^s \rangle_s = \frac{1}{Z} \sum_{s=1}^{2^N} \delta_i^s \times \exp\left\{ -\frac{1}{k_B T} \Delta G(\bar{\delta}^s) - \nu(\bar{\delta}^s) 2.303 pH \right\}. \quad (9)$$

The $(pK_a)_{i,(p)}$ is defined by the pH at which the site is half protonated. In order to find $f_i = 0.5$ the system is titrated in a predefined pH interval. In practise the partition function Z is not very neat to evaluate. The reduced site approximation [10], the multiple site transition Monte Carlo algorithm [16] or the cluster method [17] are applicable.

Provided the bulk solution is ionic, the additional salt screening has to be accounted for. If the potential of mean force is approximated by the electrostatic potential energy, the Debye–Hückel theory yields the Poisson–Boltzmann equation. A first order series expansion of the Boltzmann distributed ion charge density results in the linear Poisson–Boltzmann equation, which becomes justified for dilute solutions [18,19]. The obtained screened coulombic potential decays more rapidly than that satisfying the Poisson equation. Electrostatics and reaction field contributions are estimated by the finite difference Poisson–Boltzmann method (FDPB) [20], using the MEAD program package [1]. The lattice dimension is $81 \times 81 \times 81$ and the grid spacing is 1 Å respectively 0.25 Å at the centre of interest. The solvent accessible surface is obtained by the use of a 1.4 Å probe rolling over the Van der Waals surface of the protein. The temperature of every computation is 300 K.

The bR model structure is based on the Henderson structure (HE) [6]. The latter is a model structure built on high resolution electron microscopy data with the crystallographic resolution 3.5 Å in the membrane plane and 10 Å perpendicular to the membrane plane. The HE structure is deficient in resolving the interhelical loops and detailed side chain conformations. The structures employed in this study were constructed out of the HE model. Interhelical loops were added, the Arg 82 side chain was turned towards Asp 85, the D-helix was shifted 3 Å towards the inner side of the membrane and five internal water molecules were added [21]. Using this as an initial structure in a molecular dynamics simulation reaching equilibrium results in a stabilized structure at a root-mean-square deviation of 2.0 Å from the HE structure [21]. The new structure is henceforward referred to as the coHE structure. The coHE structure is constructed by using the GROMOS molecular dynamics package [2], and if nothing else is mentioned in the text, this atomic charge set is applied when using MEAD. The computations are performed on a Hewlett Packard HP 735 computer, and last about one central processor unit hour.

3. Results and discussion

3.1. Factors influencing the pK_a values

There are several factors in the electrostatic model of bR that are uncertain. Consequently we made a study of the pK_a sensitivity to such factors, with the

[1] The Macroscopic Electrostatics with Atomic Detail program (MEAD) version 0.2.2©1990,1992 Donald Bashford, The Scripps Research Institute, Department of Molecular Biology, La Jolla, CA 92037, USA.

[2] W.F van Gunsteren and H.J.C. Berendsen, BIOMOS B.V., University of Groningen, the Netherlands.

retinal in the all *trans* state bR_{568}. The momentous interior proton translocation residues are selected to be Arg 82; Asp 85, 96, 115, 212; Glu 204 and Lys 216 (the Schiff base: SB) [22–25]. We divide the influence factors into two categories:

1. Structural features
2. Factors related to the modelling of the electrostatics.

3.1.1. Structural features

3.1.1.1. Loops and internal water molecules. The coHE structure includes loops and five internal water molecules. The structure of loops and the positions and orientations of internal water molecules is based on modelling that may be inaccurate. It would be serious if these had large effects on the pK_a values and maybe even changed the protonation states. We excluded either loops and/or internal waters in the MEAD computations, which produced the results in Fig. 1.

The loops have small effect on Asp 85, Asp 212, Arg 82 and the Schiff base (shifting the pK_a values less or equal to about 1 unit). Asp 96 which already is protonated without loops is further stabilised in the protonated state with about 4 pK_a units when loops are included. The glutamate group 204 is clearly affected by the inclusion of the loops, but is still protonated without them. Surface calculations show that Glu 204 is exposed to the water when the loops

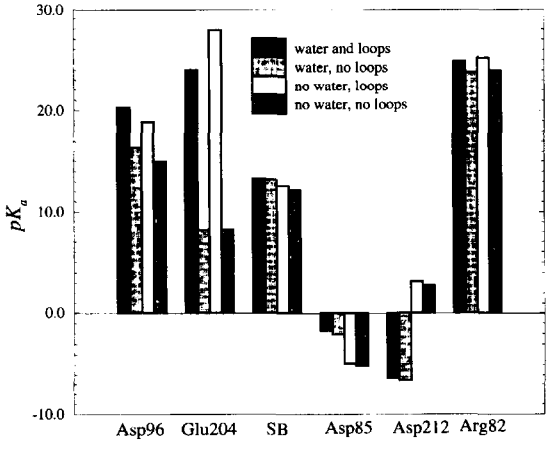

Fig. 1. The influence on the calculated pK_a values of the bR interior residues due to internal water and interhelical loops.

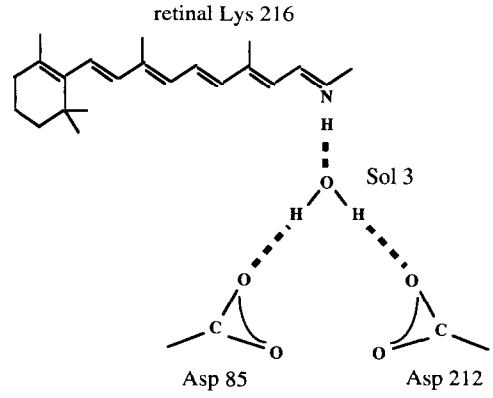

Fig. 2. The Schiff base cavity conformation including the single internal water molecule. Hydrogen bonds are represented by the dotted lines.

is removed. This explains the observed decrease of the pK_a value.

The five internal waters are abbreviated Sol 1–5 where Sol 1 and 2 are situated between Asp 96 and the Lys 216 backbone base. The third water, Sol 3, is the only one within the Schiff base cavity. It forms hydrogen bonds with the SB, Asp 85 and Asp 212 (Fig. 2), in agreement with experimental data [26,27]. Sol 4 connects Asp 212 and Arg 82 via hydrogen bonds. The last internal water, Sol 5, lies beneath Arg 82, closer to the extra cellular side. The internal waters exert great influence upon the pK_a values of Asp 85 and Asp 212 (without changing the protonation state at neutral pH) while the effect is only about 1 pK_a unit on the other residues. The charged deprotonated state of Asp 85 is destabilised with 3 pK_a units while the charged state of Asp 212 is stabilised by the internal water with 9.5 pK_a units. The inclusion of the internal water brings the pK_a of Asp 212 down clearly below the experimental upper limit 2.5 (Table 5) and is entirely due to a decrease in the ΔG_{back} terms, i.e. the water dipoles interact favourably with the Asp 212.

Water is here modelled by the empirical SPC model, having the partial charge -0.82 on the oxygen and $+0.41$ on the hydrogens. The five water molecules in the vicinity of the Schiff base, however, can hardly be considered as aqueous bulk water, and we have therefore tested the sensitivity of the results to the partial charges. As many different water charge models exist, we chose the simple Pitzer–Merrifield

Table 1
Calculated pK_a values of different internal water partial charge models

Model	Asp 96	SB	Asp 85	Asp 212	Arg 82	Glu 204
No water	18.88	12.59	−4.88	3.12	25.16	27.91
PM	19.92	12.99	−5.94	0.67	24.99	27.93
SPC	20.30	13.27	−1.69	−6.39	24.84	27.94

H_2O wave function, achieved by the SCF MO treatment with a basis set of minimal STO [34], not due to its superiority to other models, but rather because of its relevant, very different and easily obtained partial charges. The (−0.46, +0.23) partial charges are obtained by the use of population analysis [35]. With these charges applied to the water atoms we get a dipole moment of 1.28 Debye which is smaller than the vacuum value for water, 1.85 Debye, while the SPC model has the dipole moment 2.27 Debye. The results of comparison between the models are found in Table 1. As expected, the pK_a values of the PM-model are in between those without water and those with SPC-water.

3.1.1.2. Orientation of Arg 82. Henderson et al. [6] were not able to resolve the side chain orientation of Arg 82. It was placed towards the extra cellular side, but the electrostatic calculations of Bashford and Gerwert [4] suggests a cytoplasmic orientation, i.e. towards the Schiff base. This orientation gave better pK_a values. Furthermore, there was a tendency for the Arg 82 side chain to move towards the interior side in MD simulations [36]. We have above stressed the importance of internal water to stabilize the interior sites charge configuration. Sampogna and Honig [5] show that introduction of some water molecules near the Schiff base stabilizes the HE structure without the need for reorientation of Arg 82. The coHE structure has the Arg 82 side chain oriented towards the Schiff base, thus forming an ion-counterion complex together with Asp 85, Asp 212 and the protonated Schiff base. In this structure the distance between the Schiff base nitrogen and the CZ of the Arg 82 side chain is 7.8 Å. Bashford and Gerwert have a slightly smaller distance, 6.6 Å, while the distance is 12 Å in the original Henderson structure. We find, however, that during the MD-simulations this distance is even further diminished from 7.8 down to about 4 Å (see below).

3.1.1.3. Structural perturbations. The Henderson structure has some deficiency in the resolution of the atomic co-ordinates. In order to find a structure that may serve as the model structure in a computer simulation, one usually either energy minimizes or carry out a short MD simulation in accordance with some artificial force field. If the calculated pK_a values are sensitive to structural rearrangements, e.g. due to changes in protonations states, there is some difficulty in determining accurate pK_a values from both the original HE structure and the artificial model structure. For instance Sampogna and Honig [5] used bR structures corresponding to the original Henderson structure, which makes it interesting to examine how small random perturbations influences the obtained pK_a values.

A future aim is to incorporate protonation state calculations into molecular dynamics simulations. Then, short MD runs would be intervened by protonation calculations and the protonation state would change with the structure. This would make it possible to simulate enzymatic processes and entire transport cycles.

To make a prefigurative test we examined how pK_a values altered, due to random structural changes compared to changes of the same magnitude that occurred along a MD trajectory (see below). We used the coHE structure without loops, and introduced a random uniformly distributed perturbation of every atomic co-ordinate. We made 10 structures each for five root mean square perturbations rmsd in the interval of 0 to 1.0 Å. For each of them, the mean pK_a value, $\langle pK_a \rangle_{rmsd}$, and the standard deviation were calculated. The net shift $\langle pK_a \rangle_0 - \langle pK_a \rangle_{1.0}$ was about 5–10 pK_a units for the important titrating sites, except for Asp 212 which fluctuated the most. The least sensitive groups were Asp 96, Asp 115 and Arg 82 (Fig. 3). Asp 85 was fairly stable but the Schiff base and Asp 212 fluctuated a lot even for small perturbations (Fig. 4).

3.1.2. Factors related to the modelling of the electrostatics

3.1.2.1. The surroundings. The protonation state of a protein is affected by ions in the surrounding water. This is accounted for by the Poisson–Boltzmann mean field approximation. We find only a minor

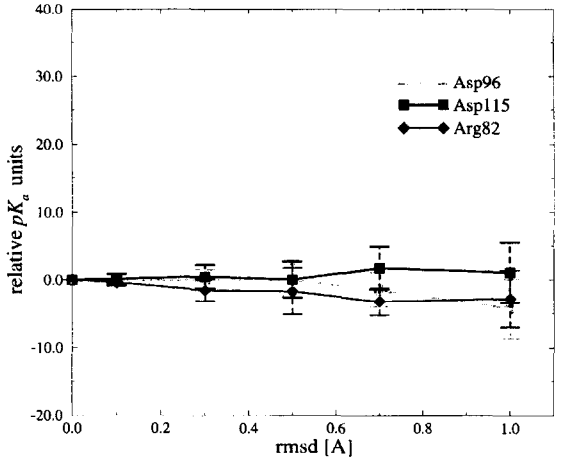

Fig. 3. The pK_a shifts of Asp 96, Asp 115 and Arg 82 due to random structural perturbations.

effect on the pK_a values of interior residues due to non zero ion concentration.

The consistency of the work by Bashford and Gerwert [4] – with membrane – and Sampogna and Honig [5] – without membrane – indicates that the lipid bilayer, modelled as a dielectric slab with the same dielectric constant as the protein molecule, only influence the pK_a values of interior residues to a small extent. We simulated the effect of the membrane on an energy minimized HE structure and the resulting pK_a shifts were ± 1–3 pK_a units, towards a stabilization of interior amino acids in the charged

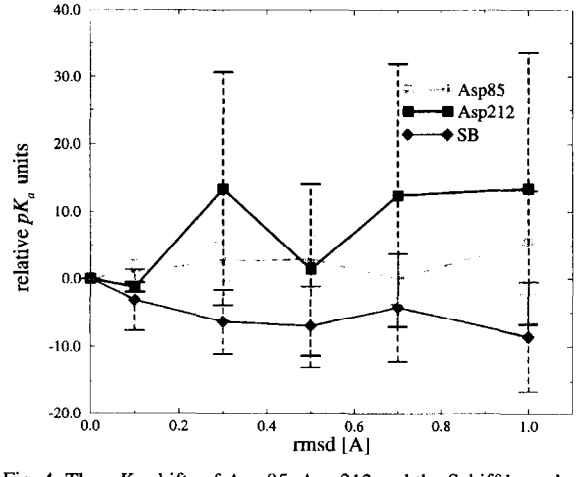

Fig. 4. The pK_a shifts of Asp 85, Asp 212 and the Schiff base due to random structural perturbations.

states. The reason for this is that the surface charges are less screened in a membrane environment, and therefore interact more strongly with other charges.

3.1.2.2. The protein permittivity. When the Poisson equation is used to determine the electrostatic potential ϕ, it is assumed that the protein has a uniform dielectric constant. There exist several different approaches to account for the electronic polarizability, stretching from ab initio treatment to more ad hoc classical methods [37]. Considering the protein as a bulk mass of uniform dielectric constant, an average value about 2–3 is obtained. This high frequency dielectric constant can not account for microscopic charge stabilization inside proteins, and leads to the prediction that all charges inside the polar medium occur in pairs with opposite sign [38]. This is easily seen from the solvation energies for inserting different charge configurations into the protein [39,40]. In proteins there is an additional screening from the permanent dipoles. When these dipoles are explicitly allowed to adjust their orientation separately according to the electrostatic environment in each protonation state – using molecular dynamics, Monte Carlo or some efficient energy minimization scheme – it is fair to use the high frequency dielectric constant. If the protein structure is treated as fixed, an increase in the effective dielectric constant is necessary. Honig et al. [41] concludes that a dielectric constant of 4 in calculations of titration curves appears reasonable.

The assumption of a uniform dielectric constant is not a trivial one, since on an atomic level it is difficult to understand if it not would be more accurate to have a varying microscopic definition, due to the local regional environment. If microscopic probes are used, $\epsilon_{\text{protein}}$ can be evaluated as a spatially varying function. Most of these attempts results in an $\epsilon_{\text{protein}} \geq 4$ [42]. Warshel and Russel [43] discuss the problem in terms of a distant dependent dielectric constant, and they find the following empirical estimate:

$$\epsilon_{\text{protein}}(r) \geq 2 + (r-1)^2,$$

with r in Å. For distances larger than 9 Å, they use the water permittivity. This approach is not valid, when the water is explicitly taken into account or considered as a region with a different dielectric

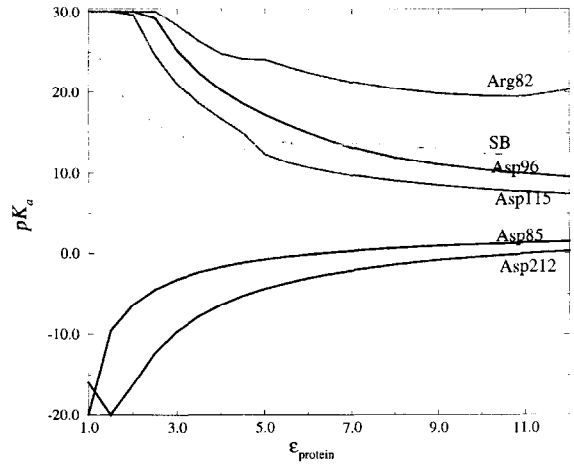

Fig. 5. The pK_a values of the bR interior residues as a function of the dielectric constant.

constant than the protein. Then the value 4 ought to be used even at long distances.

The MEAD program uses default a uniform dielectric constant of 4 in the entire protein. This choice seems to be reasonable but could certainly be called into question. To test the sensitivity of calculated pK_a values to the dielectric constant, we calculated these for the important interior residues in the coHE structure as a function of $\epsilon_{protein}$. When $\epsilon_{protein} \rightarrow 80$, i.e. the water permittivity, the pK_a values smoothly converges towards the experimental amino group acidities in water (Fig. 5). For small $\epsilon_{protein}$, the pK_a values are extremely sensitive to variations of the dielectric constant, i.e.

$$\left| \frac{\Delta(pK_a)}{\Delta\epsilon_{protein}} \right| \gg 1 \quad \text{when } \epsilon_{protein} \rightarrow 1+ .$$

This implies that $\epsilon_{protein} = 2$–3 and $\epsilon_{protein} = 4$ yield results that may differ about 10 pK_a-units. There has recently been found that calculated pK_a-values seems to be in better agreement with $\epsilon_{protein} = 20$ [44]. The reason for this is unclear. In our case this larger protein permittivity would not affect the protonation states of Arg 82, SB, Asp 85 and Asp 212. Asp 96 and Asp 115 would however decrease below 7, i.e. change into the deprotonated state in contrary to their measured pK_a-values. Hence to obtain correct pK_a values, one has to know the protein dielectric constant with fairly high accuracy.

3.1.2.3. The partial atomic charges. The coHE structure is produced by the GROMOS program package but the atomic radii and charges of MEAD are based on the polar hydrogen parameter set CHARMM19 of the CHARMM program [45]. In general the partial charges are slightly larger and more dispersed over the atoms of the site compound in the CHARMM set. Thus we applied a partial charge set that more resembles the parameter set of GROMOS. The major difference between CHARMM19 and GROMOS is the backbone dipole partial charges. The carboxy group C′O is set to (+0.55, −0.55) in CHARMM19 and (+0.35, −0.35) in GROMOS. An exchange of all backbone charges in the coHE structure to the CHARMM ones, causes a pK_a shifts of only half a pK_a unit. This change corresponds to a change of the dielectric constant for the side chain–backbone interactions from 4 to 2.5 (backbone–backbone interactions are the same in the different protonation states and thus do not influence the pK_a values). A change of the dielectric constant for all interactions from 4 to 2.5 will in contrast change the pK_a values with typically about 5 units (see Fig. 5). This illustrates that for a given fixed structure side chain–side chain interactions are much more important for the pK_a values, than side chain–backbone interactions are.

Bashford and Gerwert [4] put all the partial charges on the deprotonated Arg side chain at zero. To us, it seems more natural to have some dipoles on the Arg side chain. The effect on the important residues was small. See Tables 2 and 3. We observe a +2 pK_a shift of Arg 82. The other interior residues were not affected.

3.1.2.4. Additional titrating sites. It is understood that the Schiff base becomes deprotonated during the photo cycle of bR. The prevailing opinion is that the proton translocates to Asp 85. We have previously

Table 2
The pK_a values according to the two different deprotonated arginine states

Deprot. Arg state	Asp 96	SB	Asp 85	Asp 212	Arg 82	Glu 204
All zero	20.30	13.28	−1.66	−6.42	22.87	27.89
Dipolar	20.30	13.27	−1.69	−6.39	24.84	27.94

Table 3
The partial charge distribution of the Arg side chain

Arg state	CZ	CD	NE	HE	NH-1	HH-11	HH-12	NH-2	HH-21	HH-22	Σ
Protonated	0.50	0.10	−0.40	0.30	−0.45	0.35	0.35	−0.45	0.35	0.35	1
Deprot. all zero	0.0	0.0	0.0	0.0	0.0	0.0	0.0	0.0	0.0	0.0	0
Deprot. dipolar	0.0	0.0	−0.24	0.24	−0.48	0.24	0.24	−0.48	0.24	0.24	0

seen that internal waters play an important role in bR. One conceivable model is that one of the waters (Sol 3) that is hydrogen bonded to the Schiff-base as well as Asp 85 and Asp 212 (Fig. 2) could act as the primary proton acceptor. To test this hypothesis, we added this water as a titration site. We took the water partial charges from the PM-model and added symmetrically a third positive charge to describe the protonated state of water, H_3O^+ (The corresponding charges are −0.46, +0.487, +0.487 and +0.487.) The resulting pK_a shifts for the surrounding amino acids were less than 0.1 pK_a units and the water molecule was definitely deprotonated. Thus, the proton is certainly not at equilibrium bonded to the water molecule. However this state may still be an intermediate transition state with high free energy. The proton conductivity is governed by the rate at which the water molecule can rotate into orientations in which it can accept/donate protons and the rate at which the proton translocate from one end of a hydrogen bond to another. The high potential barrier between the Schiff base and the water molecule makes a classical proton transfer very unlikely, but proton tunnelling may occur.

The reprotonation of the Schiff base occur during the $M_{412} \rightarrow N_{550}$ transition. The general opinion is that Asp 96 donates its proton to the Schiff base via some intermediate group, perhaps internal water or Thr 89 [24,46]. It is not easy to find the pK_a value of the Threonine side chain in water solution. However we got Thr 89 protonated assuming both 20.0 and 10.0 as the site compound $(pK_a)_{i,(aq)}$ in water. This additional titrating site did not affect the important residues except for a lowering of the pK_a of Arg 82 with less than one unit.

3.2. bR dynamics

Several MD simulations of bR have recently been made by Edholm et al. [21]. Both monomer and trimer structures in vacuum and explicit water solvent, with and without lipid membrane structure. The focus of attention is the Schiff base environment of which we find the following structural features in the simulation.

- One internal water molecule (Sol 3) is tightly bound to the Schiff base hydrogen.
- The distance between the Schiff base and Asp 85 increases during the simulation from 5 to 7 Å.
- The distance between the Schiff base and Asp 212 is 3 to 4 Å.
- In the beginning of the simulation the distance between the Schiff base and Arg 82 is about 7.5 Å, but it decreases in two separate steps, first after about 195 ps to 5.5 Å and then after about 350 ps simulation to 4 Å. The final position was stable, and the system gained ~ 150 kJ/mol of electrostatic energy during this structural change.
- The distance between Arg 82 and Asp 212 decreased from 6.5 to less than 4 Å during the simulation, while the distance between Arg 82 and Asp 85 remained about 5 Å.

To examine the variation of the pK_a values along an equilibrium molecular dynamics trajectory, MEAD calculations of the pK_a values of interior residues were performed every 5:th ps during the last 400 ps

Table 4
The linear regression slope coefficients of the MD trajectory

Slope [pK_a units/ps]	Asp 96	SB	Asp 85	Asp 212	Arg 82	Glu 204
pK_{intr}	−0.0025	−0.0018	0.0021	0.00022	−0.0079	−0.0045
pK_a	−0.0023	−0.0062	0.0017	−0.017	0.0061	−0.022

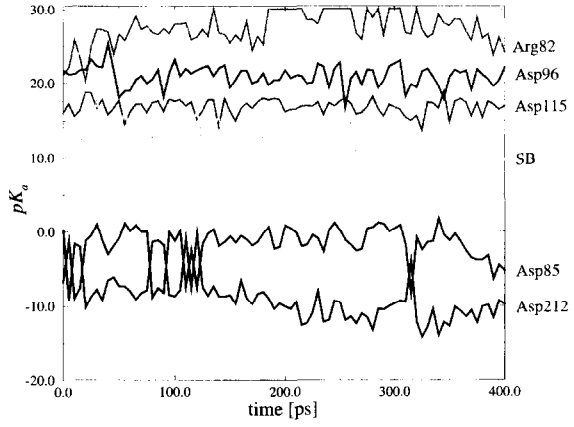

Fig. 6. The pK_a values of the bR interior residues along the MD trajectory.

of a 500 ps long MD simulation, (see Fig. 6 and Table 4). We included loops and internal water and used a single environment of aqueous solvent ($\epsilon = 80$) with zero ionic strength. We used the non zero fractional charges on the neutral Arg 82 side chain. The charges on the retinal were taken according to Edholm et al. [21] which are very similar to Bashford and Gerwert [4].

The time variation of the pK_a values are shown in Fig. 6 for the important residues. There are substantial fluctuations (about ± 3–5 pK_a units) making a pK_a value that is calculated from a snapshot structure unreliable. However there is a large gap around neutral pH, Fig. 6. This results in stable protonation states around neutral pH despite the fluctuations. The sampling time is long enough to estimate average pK_a values with a standard deviation of 1–2 pK_a units, which is good enough keeping the uncertainties in the model used in mind. In Table 5 the average pK_a values are compared with corresponding data from Bashford and Gerwert [4], Sampogna and Honig [5] and available experimental data. To describe the pK_a drift we made a curve fitting by linear regression to obtain the slope. The slope coefficients are generally small resulting in a minor drift along the MD trajectory indicating that the system is well enough equilibrated (Table 4), even though individual trajectory snapshots show more striking differences (Fig. 6). It is seen that our pK_a values tend to be in between those of Bashford and Gerwert and Sampogna and Honig except for Asp 96, Asp 115 and Glu 204 which in our case get significantly higher pK_a values than those obtained by the others. Nonetheless these residues are protonated at neutral pH. In most cases Asp 85 has a larger pK_a value than Asp 212, but there are several interchanges between the two groups (Fig. 6). The later more equilibrated interchanges are caused by a relative motion of the cavity water (Sol 3) away from Asp 212 towards the Schiff base, while it remains at a fixed distance to Asp 85. Thus the water hydrogen bond to Asp 212 is weaker, or even free, than the bond to Asp 85. This is entirely in line with experimental FTIR studies of bR [27]. The trajectory snapshot at 310 and 320 ps show pK_a(Asp 85) > pK_a(Asp 212), while at 315 ps, pK_a(Asp 85) < pK_a(Asp 212) (Fig. 7). The complex titrating behaviour of these two aspartic groups illustrates a strong coupling between them. At neutral pH both are deprotonated, while at a pH around -5 Asp 85 will in general be protonated and Asp 212 deprotonated. The proton may, however, pass over to Asp 212 for short times depending on the conformation of the protein and the

Table 5
pK_a values of some residues

Residue	Bashford et al. [4]	Sampogna et al. [5]	Present work	Experimental values
Asp 85	-3.0 ± 1.3	3 (8)	-1.9 ± 2.6	≤ 2.5
Asp 212	-16.4 ± 2	-2 (8)	-8.9 ± 3.2	≤ 2.5
Arg 82	55.1 ± 30.1	20	27.3 ± 2.2	N.A.
Asp 96	11.6 ± 1.2	9	21.0 ± 1.4	≥ 9.5
Asp 115	15.4 ± 8.6	10	16.8 ± 1.0	≥ 9.5
Schiff base	13.1 ± 13.6	21 (13)	12.4 ± 1.7	≥ 12
Glu 204	5.3 ± 1.3	-	19.8 ± 3.4	N.A.

N.A. = not available.
Experimental values from [28,29,22,30–33].
The comparison is done with the systems denoted RUD in [4] and bR_{out}(wat) in [5].

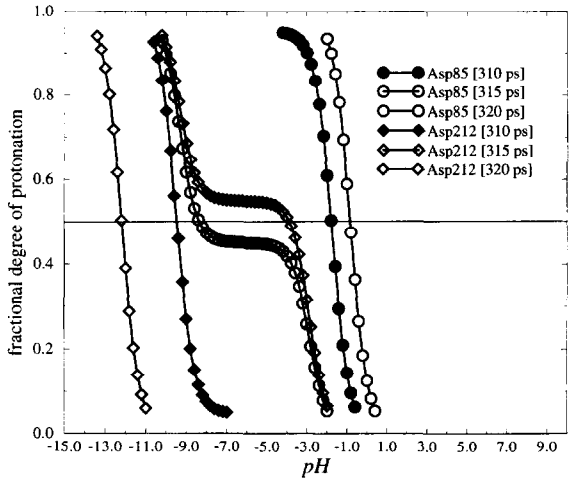

Fig. 7. The titrating behaviour of the two aspartic groups (85 and 212) at 310, 315 and 320 ps.

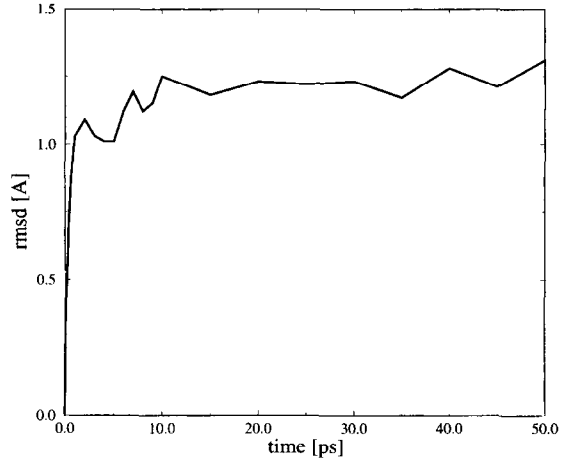

Fig. 9. The root mean square alteration of the structure as a function of time between two snapshots along the MD trajectory.

position of the intervening water. Fig. 8 shows the behaviour of Glu 204, the SB and Asp 85 groups. The Glu 204 group is clearly protonated but becomes destabilized along the trajectory, simultaneously Asp 85 approaches the unprotonated state (see Table 4). This indicates a kind of relationship between these two groups, verified in experiment [47,48]. The pK_a value of Glu 204 is considerably larger in our case than in that of Bashford and Gerwert. The reason for this is that we include the loops, which screen Glu 204 from the exterior bulk water. The resulting protonated ground state, in contrary to what Bashford and Gerwert obtain, is in agreement with recent

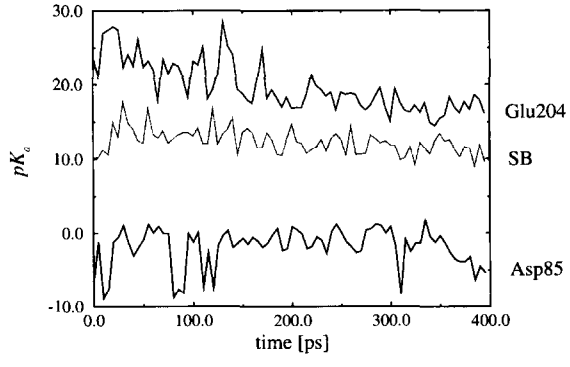

Fig. 8. The pK_a values of the SB, Glu 204 and Asp85 residues along the MD trajectory.

experimental data, although our pK_a value seems to be far too high.

The changes in pK_a values are about ten times smaller between structures taken from a MD-trajectory than between randomly perturbed structures having the same rmsd. The rmsd between MD-structures are shown as a function of separation time in Fig. 9. In order to obtain a stable pK_a value of a residue in dynamic processes of protein structures, we require the structures to be in equilibrium. If we leave the phase space trajectory, e.g. by changing the atomic co-ordinates in a random way, the pK_a values will show major shifts. This is due to the sensitivity in the electrostatic interactions terms to distance alterations.

It seems as if the intrinsic pK_a values are more stable to structural changes (Fig. 10), while even small structural alterations involving the titrating internal residues may cause very large pK_a changes. A comparison of the data shows that the pK_{intr} of Arg 82 is about zero in Bashford and Gerwert [4] ± 2.5 depending on which structure that is considered while the corresponding value is about $+6$ in the case of Sampogna and Honig [5] with a similar difference between the different conformations. We find the value $+3.7 \pm 1.5$ which is closer to the Sampogna and Honig value (Table 6). The reason for this discrepancy is the lack of dipoles on the neutral Arg 82 chain in Bashford and Gerwert. This makes the difference larger between the two forms of Arg and

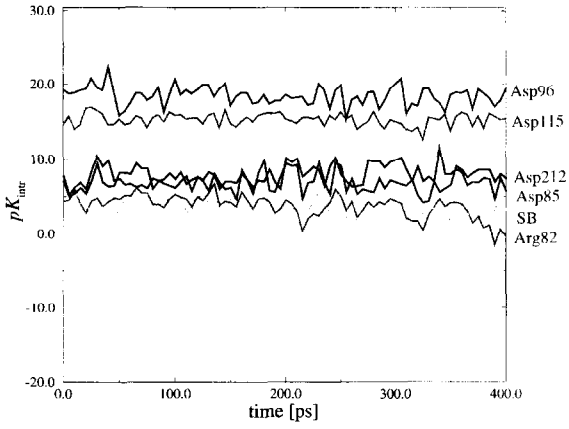

Fig. 10. The pK_{intr} values of the bR interior residues along the MD trajectory.

tends to stabilize the charged form at lower pH values. The pK_{intr} values for the aspartic acids (85, 96, 115 and 212) all agree (8–11) between Sampogna and Honig and Bashford and Gerwert. There is a slight reduction of the pK_{intr} values when explicit internal water is included in the Sampogna and Honig case. Our data agree except that we get considerably larger pK_{intr} values for Asp 96 and Glu 204. The Asp 96 group is already in the protonated state in the Bashford and Gerwert and Sampogna and Honig cases so this just leads to a further stabilization in this state. One possible reason for this may be that Asp 96, due to the presence of loops in our case, becomes more deeply buried into the interior of the protein. The higher pK_{intr} value of Glu 204 in our study results in a protonated state, in agreement with available experimental data. Finally, the Schiff base,

Table 6
pK_{intr} values of some residues

Residue	Bashford et al. [4]	Sampogna et al. [5]	Present work
Asp 85	12.4	5.9	7.7 ± 1.4
Asp 212	9.1	5.6	7.1 ± 1.4
Arg 82	-3.5	7.6	3.7 ± 1.5
Asp 96	8.3	8.6	18.4 ± 1.2
Asp 115	11.3	9.1	15.3 ± 0.8
Schiff base	-3.4	6.9	3.3 ± 1.2
Glu 204	5.1	-	15.6 ± 1.2

The comparison is done with the systems denoted RUD in [4] and bR_{out}(wat) in [5].

gets a pK_{intr} of about -3 in Bashford and Gerwert while Sampogna and Honig get about $+7$. This higher value is the reason for which Sampogna and Honig get the Schiff base protonated, even when the Arg 82 side chain is directed outwards. We get an intermediate value which in our case is sufficient for having the Schiff base protonated.

3.2.1. Sensitivity to the distance between the SB and Arg 82

Three different structures are selected $(bR)^1_{trans}$ etc., where the first represents the 7.5 Å distance to the Schiff base, the second a 5.5 Å and the third a 4.0 Å distance. We find the computed pK_a values to be in good agreement with the bR experimental values, Table 7. Returning to the result of Bashford and Gerwert [4] for the HE structure, in which they had difficulty in keeping the Schiff base protonated when the Arg side chain was oriented towards the extra cellular side. They had to fix the Schiff base in the protonated state, which means that for large separations the protonated Schiff base becomes destabilized. In the $(bR)^1_{trans}$ structure with a 7.5 Å separation, we find that the Arg side chain stabilizes the Schiff base in a protonated state. But when the Arg side chain moves closer, in the $(bR)^2_{trans}$ and $(bR)^3_{trans}$ structures, we observe a decrease in the pK_a value of the Schiff base. We conclude the closer the arginine side chain moves towards the retinal, the more the protonated Schiff base becomes destabilized. We also observed a destabilization of Glu 204 along the trajectory, i.e. a lowering of the pK_a value from about 22 at the beginning down to about 15. The pK_a shifts are larger in the first $(bR)^1_{trans}$ to $(bR)^2_{trans}$ transition than in the second one. If we concentrate on the trajectory of Arg 82 moving towards the Schiff base from the intermediate state $(bR)^2_{trans}$ to the final stable state $(bR)^3_{trans}$ we find a distance alteration about 1.5 Å. Fig. 6

Table 7
pK_a values of the three all *trans* structures

	Distance	Asp 96	SB	Asp 85	Asp 212	Arg 82	Glu 204
$(bR)^1_{trans}$	7.5	20.3	13.3	-1.7	-6.4	24.8	27.9
$(bR)^2_{trans}$	5.5	20.5	9.4	-4.6	-10.7	26.1	17.1
$(bR)^3_{trans}$	4.0	19.1	9.4	-5.6	-12.4	25.4	15.3

Table 8
Average pK_a values over the three *trans* structures in Table 7 and the corresponding *cis* structures obtained in slow and fast conversions

	Asp 96	SB	Asp 85	Asp 212	Arg 82	Glu 204
$\langle (bR)_{trans} \rangle_{1-3}$	20.0 ± 0.8	10.7 ± 2.3	-4.0 ± 2.0	-9.8 ± 3.1	25.4 ± 0.7	20.1 ± 6.8
$\langle (bR)_{cis,\text{slow}} \rangle_{1-3}$	21.6 ± 1.6	11.4 ± 3.4	-3.4 ± 1.4	-10.8 ± 2.6	27.7 ± 1.5	15.0 ± 2.3
$\langle (bR)_{cis,\text{forced}} \rangle_{1-3}$	21.5 ± 2.6	11.2 ± 1.5	-2.6 ± 1.4	-9.5 ± 0.4	27.8 ± 1.4	18.3 ± 5.0
$\langle (\Delta pK_a)_{\text{forced}} \rangle$	$+1.5 \pm 1.9$	$+0.6 \pm 1.5$	$+1.4 \pm 1.0$	$+0.4 \pm 3.1$	$+2.4 \pm 1.9$	-1.8 ± 2.4

shows no major shifts in any sites during 350–370 ps, except for a possible lowering of the Asp 85 value. Not even in Arg 82, which moves at least 1.5 Å. The total electrostatic energy gain for the system is about 70 kJ/mol, which is strange to say not seen in the pK_a values. However since Arg 82 moves closer to Asp 212 and the Schiff base and Asp 85 moves away from SB while it remains fixed to Arg 82, we find that the slopes (Table 4) confirm Arg 82 and Asp 212 to be stabilized in the charged state and Asp 85 and SB to be destabilized towards the neutral state.

3.2.2. The retinal isomerization

Several attempts have been made to simulate parts of the bR photocycle [49–51]. Some involving computed pK_a predictions of the proton translocation residues [5,8,7]. When the retinal absorbs a photon, the normal bR_{568} all *trans* state becomes the excited J_{625} all *trans* state. This excited state can not be properly simulated by a classical MD potential energy function. We will use a model in which we perturb the J_{625} state into the K_{590} state by altering the potential, thus forcing the dihedral to isomerize into the C_{14}/C_{15}-*cis* state [51]. We make the conversion both fast (500 fs) and a bit more slowly (10 ps) to allow for some equilibration. To get statistics we convert all of the three all *trans* structures for which pK_a-values are reported in Table 7. The averages and standard deviations of the pK_a values and pK_a shifts are given in Table 8. As seen there are no significant pK_a alterations, except for Glu 204 which pK_a value is lowered about 5 units in the slow isomerization. This is not enough for changing the protonation state. However since the proton release take place much later in the photo cycle a further relaxation of the protein, in which the proton translocates from the Schiff base to Asp 85, is probably necessary in order to find a protein conformation with a pK_a value lower than 7.

It should be emphasised that these calculations of the pK_a isomerization shifts only involve the electrostatic interactions of fixed Schiff base partial charges. Steric effects and the great polarizability of the π electrons making the SB susceptible to charge redistribution along the polyene chain [52], which may affect the intrinsic pK_a, are not included in this model as mentioned by Engels et al. [7].

4. Conclusions

The electrostatic contribution to the pK_a values of the proton translocating residues in bacteriorhodopsin along a 400 ps molecular dynamics trajectory was calculated. The sensitivity to structural factors and factors related to the modelling of the electrostatics was studied. We conclude that the inclusion of counter ions, membrane and the choice of partial atomic charges do not influence the results significantly. The interhelical loops screen Glu 204 from the surrounding water, resulting in an increase of the pK_a value. The other residues are less influenced by the loops.

On the other hand, the choice of protein dielectric constant in the range of 2 to 4 has a large influence on the pK_a values of the important interior residues. The calculated pK_a values may differ up to about 10 units depending on the selected $\epsilon_{\text{protein}}$ in this interval.

We find in agreement with other authors [5,49,50,7] that it is important to include internal water molecules in the vicinity of the Schiff base cavity. These waters stabilize the interior ion-counter ion complex. This is unambiguous for Asp 212, the pK_a value of which is lowered 10 pH-units clearly

below the experimental upper limit, if internal waters are included. It is not sufficient to include these internal waters in a continuum approximation as e.g. by Bashford and Gerwert [4].

One single water molecule is bound between the Schiff base, Asp 212 and Asp 85. This one might be especially important for the electrostatics. To investigate this, it was included as an additional titration site. The electrostatic calculations show clearly that this water remains neutral and is not at equilibrium in the protonated (charged) state. This water may, however, still be important for the proton translocation, but then after conformational changes in the protein or as a part in a fast non-equilibrium process.

Random variations of the protein structure causes large pK_a perturbations (about 5–15 units) even if the resulting structural changes correspond to rmsd values of only about 1 Å. Changes in structure resulting in similar rmsd values occur in a few ps along an equilibrium MD trajectory, which however only results in fluctuations of about ± 2 pK_a units. This may still be crucial if one is interested in accurate results. In the bR case which is studied here, the pK_a of all important residues are well separated from 7. So at pH 7 there are no problems. However at other (more unrealistic) pH values these fluctuations may be important. For example there are several interchanges of pK_a values between Asp 85 and Asp 212 along the trajectory which means that at pH values around -5 these two residues will share one proton that momentarily will pass between them.

During the MD run arginine 82 moves closer to the Schiff base resulting in a destabilization of the protonated SB but a further stabilization of the charge states of the aspartic acid group 212. The Asp 85 (unprotonated) and Glu 204 (protonated) groups become destabilized, i.e. they approach the protonated state respectively the unprotonated state. This indicates a relationship between these groups.

We do not see any significant pK_a alterations of the titratable sites when the chromophore is isomerized in either a fast (0.5 ps) or in a slower way (10 ps). An exception is Glu 204. Brown et al. [25] suggest that Glu 204 is the terminal proton release group. The pK_a value of Glu 204 decreases by 5 units during the *trans/cis* isomerization, which is not sufficient to obtain the charged unprotonated state. However, the proton release occurs in a much later stage of the photo cycle. A further relaxation of the protein *cis* state, with the proton translocated from the Schiff base to Asp 85, is probably necessary to get into a conformation with a pK_a value of Glu 204 below 7.

Acknowledgements

We thank Fritz Jähnig and Jochen Nagel for valuable comments and a special thanks to Donald Bashford for access to the MEAD program.

References

[1] J. Warwicker and H.C. Watson, Calculation of the electric potential in the active site cleft due to α-helix dipoles, J. Mol. Biol., 157 (1982) 671–679.

[2] M.K. Gilson and B.H. Honig, Calculation of electrostatic potentials in an enzyme active site, Nature (London), 330 (1987) 84–86.

[3] D. Bashford and M. Karplus, pK_a's of ionizable groups in proteins: atomic detail from a continuum electrostatic model, Biochemistry, 29 (1990) 10219–10225.

[4] D. Bashford and K. Gerwert, Electrostatic calculations of the pK_a values of ionizable groups in bacteriorhodopsin, J. Mol. Biol., 224 (1992) 473–486.

[5] R.V. Sampogna and B. Honig, Environmental effects on the protonation states of active site residues in bacteriorhodopsin. Biophys. J., 66 (1994) 1341–1352.

[6] R. Henderson, J.M. Baldwin, T.A. Ceska, F. Zemlin, E. Beckmann and K.H. Downing, Model for the structure of bacteriorhodopsin based on high-resolution electron cryomicroscopy, J. Mol. Biol., 213 (1990) 899–929.

[7] M. Engels, K. Gerwert and D. Bashford, Computational studies of the early intermediates of the bacteriorhodopsin photocycle, Biophys. Chem., 56 (1995) 95–104.

[8] C. Scharnagl, J. Hettenkofer and S.F. Fischer, Electrostatic and conformational effect on the proton translocation steps in bacteriorhodopsin: Analysis of multiple M structures. J. Phys. Chem., 99 (1995) 7787–7800.

[9] C. Lim, D. Bashford and M. Karplus, Absolute pK_a calculations with continuum dielectric methods, J. Phys. Chem., 95 (1991) 5610–5620.

[10] D. Bashford and M. Karplus, Multiple-site titration curves of proteins: an analysis of exact and approximate methods for their calculation, J. Phys. Chem., 95 (1991) 9556–9561.

[11] A. Yang, M.R. Gunner, R. Sampogna, K. Sharp and B. Honig, On the calculation of pK_as in proteins, Proteins, 15 (1993) 252–265.

[12] C. Tanford and R. Roxby, Interpretation of protein titration curves. Application to lysozyme, Biochemistry, 4 (1972) 2192–2198.

[13] J.G. Kirkwood, Theory of solutions of molecules containing widely separated charges with special application to zwitterions, J. Chem. Phys., 2 (1934) 351–361.
[14] H.L. Friedman, Image approximation of the reaction field, Mol. Phys., 29 (1975) 1533–1543.
[15] R. Abagyan and M. Totrov, Biased probability Monte Carlo conformational searches and electrostatic calculations for peptides and proteins, J. Mol. Biol., 235 (1994) 983–1002.
[16] P. Beroza, D.R. Fredkin, M.Y. Okamura and G. Feher, Protonation of interacting residues in a protein by a Monte Carlo method: application to lysozyme and the photosynthetic reaction center of Rhodobacter sphaeroides, Proc. Natl. Acad. Sci. USA, 88 (1991) 5804–5808.
[17] M.K. Gilson, Multiple-site titration and molecular modelling: two rapid methods for computing energies and forces for ionizable groups in proteins. Proteins, 15 (1993) 266–282.
[18] D.A. McQuarrie, Statistical Mechanics, Harper Collins, New York, 1976.
[19] A. Prock and G. McConkey, Topics in Chemical Physics, based on the Harvard lectures of Peter Debye, Elsevier, New York, 1962.
[20] A. Nicholls and B. Honig, A rapid finite difference algorithm, utilizing successive over-relaxation to solve the Poisson-Boltzmann equation, J. Comp. Chem., 12 (1991) 435–445.
[21] O. Edholm, O. Berger and F. Jähnig, Structure and Fluctuations of Bacteriorhodopsin in the Purple Membrane: A molecular dynamics study, J. Mol. Biol., 250 (1995) 94–111.
[22] S. Subramaniam, T. Marti and H.G. Khorana, Protonation state of Asp (Glu)-85 regulates the purple-to-blue transition in bacteriorhodopsin mutants Arg-82 → Ala and Asp-85 → Glu: The blue form is inactive in proton translocation, Proc. Natl. Acad. Sci USA, 87 (1990) 1013–1017.
[23] H. Otto, T. Marti, M. Holz, T. Mogi, L. Stern, F. Engel, H.G. Khorana and M.P. Heyn, Substitution of amino acids Asp-85, Asp-212, and Arg-82 in bacteriorhodopsin affects the proton release phase of the pump and the pK of the Schiff base, Proc. Natl. Acad. Sci USA, 87 (1990) 1018–1022.
[24] R.A. Mathies, S.W. Lin, J.B. Ames and W.T. Pollard, From femtoseconds to biology: mechanism of bacteriorhodopsin's light-driven proton pump, Annu. Rev. Biophys. Biophys. Chem., 20 (1991) 491–518.
[25] L.S. Brown, J. Sasaki, H. Kandori, A. Maeda, R. Needleman and J.K. Lanyi, Glutamic acid 204 is the terminal proton release group at the extracellular surface of bacteriorhodopsin, J. Biol. Chem., 270 (1995) 27122–27126.
[26] R.R. Birge and C. Zhang, Two-photon double resonance spectroscopy of bacteriorhodopsin. Assignment of the electronic and dipolar properties of the low-lying $^1A_g*^-$-like and $^1B_u*^+$-like π, $\pi*$ states, J. Chem. Phys., 92 (1990) 7178–7195.
[27] H. Kandori, Y. Yamazaki, J. Sasaki, R. Needleman, J.K. Lanyi and A. Maeda, Water-mediated proton transfer in proteins: an FTIR study of bacteriorhodopsin, J. Am. Chem. Soc., 117 (1995) 2118–2119.
[28] M. Engelhard, K. Gerwert, B. Hess, W. Kreutz and F. Siebert, Light-driven protonation of changes of internal aspartic acids of bacteriorhodopsin: An investigation by static and time-resolved infrared difference spectroscopy using [4-^{13}C]aspartic acid labeled purple membrane, Biochemistry, 24 (1985) 400–407.
[29] K. Gerwert, U.M. Ganter, F. Siebert and B. Hess, Only water-exposed carboxyl groups are protonated during the transition to the cation-free bacteriorhodopsin, FEBS Lett., 213 (1987) 39–44.
[30] J. Herzfeld, S.K. Das Gupta, M.R. Farrar, G.S. Harbison, A.E. McDermott, S.L. Pelletier, D.P. Raleigh, S.O. Smith, C. Winkel, J. Lugtenburg and R.G. Griffin, Solid-state ^{13}C NMR study of tyrosine protonation in dark-adapted bacteriorhodopsin, Biochemistry, 29 (1990) 5567–5574.
[31] S. Druckmann, M. Ottolenghi, A. Pande, J. Pande and R.H. Callender, Acid-base equilibrium of the Schiff base in bacteriorhodopsin, Biochemistry, 21 (1982) 4953–4959.
[32] A. Lewis, M.A. Marcus, B. Ehrenberg and H. Crespi, Experimental evidence for secondary protein chromophore interactions at the Schiff base linkage in bacteriorhodopsin: molecular mechanism for proton pumping, Proc. Natl. Acad. Sci. USA, 75 (1978) 4642–4646.
[33] A.G. Doukas, A. Pande, T. Suzuki, R.H. Callender, B. Honig and M. Ottolenghi, On the mechanism of hydrogen-deuterium exchange in bacteriorhodopsin, Biophys. J., 33 (1981) 275–280.
[34] R.M. Pitzer and D.P. Merrifield, Minimum basis wavefunctions for water, J. Chem. Phys., 52 (1970) 4782–4787.
[35] I.N. Levine, Quantum Chemistry, fourth edition. Prentice Hall, New Jersey, 1991.
[36] O. Edholm and F. Jähnig, Molecular dynamics simulations of bacteriorhodopsin, in A. Pullman et al. (Eds.), Membrane Proteins: Structures, Interactions and Models, Kluwer, Amsterdam, 1992, p. 69–84.
[37] K.A. Sharp and B. Honig, Electrostatic interactions in macromolecules: theory and applications, Annu. Rev. Biophys. Biophys. Chem., 19 (1990) 301–332.
[38] B.H. Honig and W.L. Hubbell, Stability of salt bridges in membrane proteins, Proc. Natl. Acad. Sci. USA, 81 (1984) 5412–5416.
[39] M. Born, Volumen und Hydrationswärme der Ionen. Z. Phys., 1 (1920) 45–49.
[40] L. Onsager, Electric moments of molecules in liquids, J. Am. Chem. Soc., 58 (1936) 1486–1493.
[41] B.H. Honig, W.L. Hubbell and R.F. Flewelling, Electrostatic interactions in membranes and proteins, Annu. Rev. Biophys. Biophys. Chem., 15 (1986) 163–193.
[42] A. Warshel and J. qvist, Electrostatic energy and macromolecular function, Annu. Rev. Biophys. Biophys. Chem., 20 (1991) 267–298.
[43] A. Warshel and S.T. Russel, Calculations of electrostatic interactions in biological systems and in solutions, QRB., 17 (1984) 283–422.
[44] J. Antosiewicz, J.A. McCammon and M.K. Gilson, The determinants of pK_as in proteins, Biochemistry, 35 (1996) 7819–7833.
[45] B.R. Brooks, R.E. Bruccoleri, B.D. Olafson, D.J. States, S.

Swaminathan and M. Karplus, CHARMM: a program for macromolecular energy minimization, and dynamics calculations, J. Comp. Chem., 4 (1983) 187–217.

[46] J. le Coutre, J. Tittor, D. Oesterhelt and K. Gerwert, Experimental evidence for hydrogen-bonded network proton transfer in bacteriorhodopsin shown by Fourier-transform infrared spectroscopy using azide as catalyst, Proc. Natl. Acad. Sci. USA, 92 (1995) 4962–4966.

[47] S.P. Balashov, R. Govindjee, E.S. Imasheva, S. Misra, T.G. Ebrey, Y. Feng, R.K. Crouch and D.R. Menick, The two pK_a's of aspartate-85 and control of thermal isomerization and proton release in the arginine-82 to lysine mutant of bacteriorhodopsin, Biochemistry, 34 (1995) 8820–8834.

[48] S.P. Balashov, E.S. Imasheva, R. Govindjee and T.G. Ebrey, Titration of aspartate-85 in bacteriorhodopsin: What it says about chromophore isomerization and proton release, Biophys. J., 70 (1996) 473–481.

[49] F. Zhou, A. Windemuth and K. Schulten, Molecular dynamics study of the proton pump cycle of bacteriorhodopsin, Biochemistry, 32 (1993) 2291–2306.

[50] W. Humphrey, I. Logunov, K. Schulten and M. Sheves, Molecular dynamics study of bacteriorhodopsin and artificial pigments, Biochemistry, 33 (1994) 3668–3678.

[51] J. Nagel, Molekulardynamische Simulationen zum Photozyklus von Bacteriorhodopsin, Diplomarbeit der Fakultät für Physik der Eberhard-Karls-Universität Tübingen, 1995.

[52] P. Tavan, K. Schulten and D. Oesterhelt, The effect of protonation and electrical interactions on the stereochemistry of retinal Schiff bases, Biophys. J., 47 (1985) 415–430.